Alterations of EDEM1 functions enhance ATF6 pro-survival signaling

Alexandra Papaioannou, Arisa Higa, Gwenaele Jegou, Florence Jouan, Raphael Pineau, Laure Saas, Tony Avril, Olivier Pluquet, Eric Chevet

Received Date : 12-Jul-2017

Revised Date : 31-Aug-2018

Accepted Date : 28-Sep-2018

Alterations of EDEM1 functions enhance ATF6 pro-survival signaling

Alexandra Papaioannou[1,2,*], Arisa Higa[1,*,†], Gwénaële Jégou[1,2], Florence Jouan[1,2], Raphael Pineau[1,2], Laure Saas[3], Tony Avril[1,2], Olivier Pluquet[3] and Eric Chevet[1,2,3**]

[1]INSERM U1242 ; Université de Rennes, Rennes, France. [2]Centre de Lutte Contre le Cancer Eugène Marquis, Rennes, France. [3]Univ. Lille, CNRS, Institut Pasteur de Lille, UMR8161 – M3T – Mechanisms of Tumorigenesis and Targeted Therapies, F-59000 Lille, France.

Running title: ER glycoprotein quality control and ATF6 signaling

Article type : Original Articles

*equal contribution

[†]Present address : Medical-Industrial Translational Research Center, Fukushima Medical University.

**Correspondance to: EC – « Proteostasis and Cancer » team, Inserm U1242, Centre de Lutte contre le cancer Eugène Marquis, Avenue de la bataille Flandres Dunkerque, 35042 Rennes, France. Email: eric.chevet@inserm.fr.

Keywords: Endoplasmic Reticulum quality control, cancer, Unfolded Protein Response

Abstract

Activating transcription factor 6 alpha (referred to as ATF6 hereafter) is an endoplasmic reticulum (ER)-resident glycoprotein and one of the 3 sensors of the unfolded protein response (UPR). Upon ER stress, ATF6 is exported to the Golgi complex where it is cleaved by the S1P and S2P proteases thus releasing ATF6 cytosolic fragment and leading to the transcription of ATF6 target genes. In this study, we performed a phenotypic small interfering RNA (siRNA) screening to better characterize the ER mechanisms involved in ATF6 activation upon ER stress. This revealed that silencing of ER-degradation enhancing alpha-mannosidase-like protein-1 (EDEM1) increased the bioavailability of ER stress-induced ATF6 export to the Golgi complex through the stabilization of the natively unstable ATF6 protein. Moreover, we characterized a somatic variant of EDEM1 (N198I) found in hepatocellular carcinoma that alters ATF6 signaling and might provide a selective advantage to the transforming cells. Hence, our work confirms the natively unstable nature of ATF6 and links this property to potentially associated pro-oncogenic functions.

List of abbreviations

ATF6: activating transcription factor 6
EDEM1: ER degradation-enhancing alpha-mannosidase-like protein 1
IRE1: inositol-requiring enzyme-1
PERK: PKR-like endoplasmic reticulum kinase
XBP1: X-box-binding protein 1
UPR: unfolded protein response
ERQC: ER quality control
ERAD: ER-associated degradation
RIDD: regulated IRE1-dependent decay
CST: castanospermine
KIF: kifunensine

.

HCC: hepatocellular carcinoma

Introduction

The unfolded protein response (UPR) is an adaptive pathway that either allows the cells to overcome endoplasmic reticulum (ER) stress or promote cell death in the case of overwhelming misfolding burden [1]. Three ER resident proteins, namely the protein kinase PKR-like ER kinase (PERK), the inositol-requiring enzyme-1 alpha (referred to as IRE1 hereafter) and the activating transcription factor 6 alpha (referred to as ATF6 hereafter) are the major transducers of the UPR in mammals. They display an ER-luminal domain that senses misfolded proteins and are activated by a common mechanism involving the dissociation of the ER chaperone BIP/GRP78. PERK is responsible for translational attenuation through the phosphorylation of the alpha subunit of the eukaryotic translation initiation factor-2 alpha (eIF2α) [2]. IRE1, mediates the unconventional splicing of X-box-binding protein 1 (*Xbp1*) mRNA together with the tRNA ligase RtcB [3, 4, 5], promotes degradation of mRNA and microRNA through regulated IRE1-dependent decay (RIDD; [6]) and controls JNK activation [7]. The third arm of the UPR is controlled by ATF6. This membrane-anchored transcription factor is an ER resident type II transmembrane protein regulated by intra-membrane proteolysis by the Golgi apparatus localized site-1 and site-2 proteases (S1P and S2P) upon ER stress [8]. Recently, it was demonstrated that the ER folding machinery and in particular protein disulfide isomerases (PDIs) were involved in the activation and/or deactivation process of the three ER stress sensors [9, 10]. Moreover, ATF6 was identified as a natively unstable protein [11], possibly due to the presence of intrinsically disordered regions in its luminal domain, and degraded through proteasomal dependent mechanisms [12]. ATF6 is classified as an ER-associated degradation (ERAD)-Lm (m=membrane) substrate and the only one in its class to require for its degradation both mannose trimming and the ERAD component SEL1L [13]. Despite this evidence, the precise molecular mechanisms controlling ATF6 activation in the ER remain to be further characterized.

To further investigate the relationships between the molecular machines regulating ER protein quality control (ERQC) and ATF6 activation processes in this compartment, we developed a functional ATF6 ER export screen using small interfering RNA (siRNA) targeting a panel of well-established ERQC components [14]. Our data highlight the essential contribution of ER glycoprotein quality control mechanisms in the control of ATF6 activation upon ER stress and point towards EDEM1 as a key component of this pathway. To further link this observation to pathophysiology, we took advantage of the recent

.

identification of a somatic mutation in EDEM1 (N198I) that is associated with the development of hepatocellular carcinoma (HCC) [15, 16]. We show that expression of the EDEM1 N198I affects ATF6 activation pattern compared to EDEM1 wild-type under basal conditions thus pre-conditioning cells to better cope with ER stress. In the context of cancer development, we propose that this mechanism could therefore provide a selective advantage to the mutant cells over their wild-type counterparts.

Results

ATF6 export from the ER upon ER stress - ATF6 is a 90-kDa ER-resident protein and is cleaved to a 50-kDa protein by S1P and S2P proteases in the Golgi apparatus upon ER stress to activate UPR signaling [8]. To confirm whether this phenomenon could be reproduced in our experimental system, we treated HeLa cells with three well-known ER stress-inducing chemicals, namely dithiothreitol (DTT, a reducing agent), thapsigargin (Tg, an inhibitor of ER Ca^{2+}-ATPase) or tunicamycin (Tun, a N-glycosylation inhibitor). Cell lysates were extracted and analyzed by immunoblotting using anti-ATF6 antibody. Full length ATF6 (ATF6-p90, black arrowhead) was detected under non-ER stress conditions and active form of this protein (p50-ATF6, white arrowhead) appeared from 30 min after treatment of DTT (**Figure 1A**). ATF6 cleavage was also found in the cells treated with Tg and Tun. Consistent with the previous reports [8, 10, 12, 17, 18], the non-glycosylated form of p90-ATF6 was detected in Tun-treated cells (**Figure 1A**, asterisk). Furthermore, we found that DTT was the strongest inducer of ATF6 activation. ATF6 is a short-lived protein with 2 h of half-life [8], and is degraded by the ubiquitin-proteasome system [12]. To test if proteasome inhibition could attenuate the degradation of ATF6 in our experimental condition, HeLa cells were treated with MG132. This analysis showed that MG132 treatment caused the stabilization of p90-ATF6 but not its activation (**Figure 1B**). In the same settings, following treatment with MG132 for 4h, cells were further treated with DTT, Tg or Tun. After exposure to ER stress, whole cell extracts were prepared and applied to SDS-PAGE and immunoblotting. This revealed that pretreatment with MG132 enhanced the activation of ATF6 upon ER stress (along with its expression) compared to ER stress alone (**Figure 1C**). Immunofluorescence analysis was also carried out using HeLa cells transiently expressing FLAG-tagged ATF6 protein and DTT as an ER stressor in order to confirm the results in Figure 1C. Confocal microscopy analysis revealed that fluorescence signals of ATF6 proteins were observed in the perinuclear region of the cells treated with MG132 or vehicle (DMSO) alone and were translocated to the nucleus upon DTT treatment (**Figure 1D**). When HeLa cells were pretreated with MG132 prior to addition of DTT, higher level of ATF6

.

fluorescence accumulated in the nucleus compared to cells subjected to DTT alone (**Figure 1D**), thereby confirming the immunoblot results. These data indicate a close relationship between ER-associated degradation (ERAD) and ATF6 activation process and confirm the natively unstable nature of ATF6.

Identification of EDEM1 as a regulator of ATF6 activation upon ER stress - To further document the molecular mechanisms linking ERQC/ERAD and ATF6 activation, we designed a cell-based siRNA assay against ERQC/ERAD components. Forty-eight hours post-siRNA transfection, the cells were further transfected with the FLAG-ATF6. Twenty-four hours later, the cells were treated with DTT for 2h to induce ER stress. These cells were then immuno-stained using anti-FLAG and anti-CNX (ER marker) or anti-Giantin (Golgi complex marker) antibodies as described previously [10]. Cells expressing FLAG-ATF6 protein (number of cells counted ranged from 669 and 22034; **Figure 2A**) were analyzed for the presence of FLAG-ATF6 in the ER, Golgi complex and nucleus. The percentage of cells displaying both Golgi and nuclear localization of FLAG-ATF6 in each siRNA-transfected cell population was determined and compared to the control siRNA-transfected cells (**Figure 2A**; primary screen). Among the various ERQC components, only EDEM1 and SEC61alpha were validated in a second screen to indeed affect ATF6 export upon their silencing. As such EDEM1 knock-down led to increased ATF6 export, while SEC61alpha to decreased export of ATF6 to the Golgi complex upon DTT treatment (**Figure 2B**; siRNA-1 for primary screen, siRNA-2 (green) for validation screen). To confirm the effect of both EDEM1 siRNAs on their cognate target, we transfected each siRNA into HeLa cells and examined endogenous EDEM1 expression using immunoblot (**Figure 2C**). Transfection of each siRNA (siRNA-1 and siRNA-2) led to significant decrease in EDEM1 expression compared to control siRNA. Both siRNAs neither impacted CNX nor ERK1 expression used as loading standards (**Figure 2C**). ER stress-induced ATF6 activation was also monitored using immunoblotting in HeLa cells. This revealed that silencing of EDEM1 using the siRNAs tested in the screen enhanced ATF6 cleavage upon DTT treatment (**Figure 2D**; white arrowheads), thus confirming the immunofluorescence data. EDEM1 silencing also led to the stabilization of the full-length ATF6 as soon as 30 min after DTT treatment, an effect also observed upon treatments with Tg and Tun (**Figure 2D**). These data show that EDEM1 contributes to ATF6 stabilization, and thus activation upon ER stress.

.

EDEM1 silencing enhances ATF6 transcriptional activity - To further demonstrate the effect of EDEM1 silencing on ATF6 activation and the subsequent impact on the transcriptional activation of ATF6 target genes, we measured the expression levels of ATF6 target genes encoding mRNA in control and EDEM1-silenced cells following DTT treatment (1mM) using quantitative RT-PCR (q-PCR). First, we confirmed that the expression of *Edem1* mRNA was attenuated by siRNA–mediated silencing in both HeLa cells (**Figure 3A**) and normal human dermal fibroblasts (NHDFs) (**Figure 3B**). Then we analyzed the expression of four ATF6 *bona fide* target genes (*Ero1Lβ*, *Grp94*, *Orp150* and *Herpud1*) [19, 20] in Hela cells (**Figure 3C**) and the same genes plus four UPR target genes (spliced form of *Xbp1* (*Xbp1s*), *Chop*, *Atf4*, *Gadd34*) in NHDFs upon DTT induced stress and/or silencing of EDEM1 (**Figure 3D**). This revealed that EDEM1 silencing increased the induction of ATF6 target genes upon ER stress without affecting the induction of other UPR targets, such as *Xbp1s, Chop* and *Gadd34* (**Figure 3C-D**). Interestingly, dose-response with DTT indicated that EDEM1-silenced NHDFs were selectively more sensitive than their non-transfected counterparts for the induction of *Orp150* mRNA (**Figure 3E**). Finally, *Ero1Lβ* mRNA expression in NHDFs following DTT treatment differed from that observed in HeLa. This might be indicative of differential redox control between primary cells (NHDFs) and tumor cells (HeLa). Overall, these data show that the effects of EDEM1 silencing on ATF6 activation are conserved in both established cell lines and primary cells in culture thus reinforcing the importance ERQC/ERAD in ATF6 biology.

Mechanisms of EDEM1-mediated ATF6 regulation - Our results showed that EDEM1 silencing enhances the accessibility of ATF6 activation upon ER stress. As EDEM1 has been involved in ERQC/ERAD for glycoproteins, our results suggested that glycan-dependent ERQC/ERAD mechanisms might be actively involved in the ATF6 activation process most likely in the export from the ER phase. To this end, DTT-mediated activation of ATF6 was tested in the presence or absence of the ER alpha mannosidase I inhibitor, kifunensine (KIF) or of the glucosidase I/II inhibitor, castanospermine (CST). This revealed that KIF enhanced ATF6 activation upon DTT treatment (**Figure 4A**) whereas CST reduced it (**Figure 4B**), thereby confirming that ATF6 glycosylation could be of importance for its activation. The stability of p90-ATF6 was also investigated in response to DTT and upon KIF or CST and DTT treatment (**Figure 4C**). This confirmed that CST treatment increased the stability of ATF6-p90 upon DTT treatment whereas KIF treatment reduced it. These results were confirmed by the analysis of the induction of two ATF6 target genes *Grp94* and *Herpud1*. Indeed, KIF treatment promoted DTT-mediated induction of both *Grp94* and *Herpud1* mRNA, whereas CST treatment reduced it (**Figure 4D**). KIF and CST alone did not

.

impact on the expression of those genes (**Figure 4D**). To test whether EDEM1 could act on the stability of ATF6, we determined the half-life of newly synthesized ATF6 under basal conditions upon silencing of EDEM1 or upon treatment with KIF, separately (**Figure 4E**). Quantification analyses revealed that either upon EDEM1 silencing or upon KIF treatment, the stability of ATF6 was increased (**Figure 4F**). Collectively, these results suggest a tight control of ATF6 availability for activation upon ER stress that is regulated by glycosylation on ATF6.

EDEM1 N198I affects ATF6 activation upon ER stress - ATF6 has already been reported to play an indirect role in hepatocarcinogenesis [21, 22], however the underlying mechanisms still remain uncharacterized. Interestingly, a somatic EDEM1 mutation, N198I (indicated by a grey circle in **Figure 5A**), was identified in hepatocellular carcinoma (HCC) tumors, and specifically in 1 out of 24 samples after whole-exome sequencing analysis with predicted functional consequences [15]. This mutation was found also in another study in 2 tumors out of 243 sequenced [16]. Based on the effect of EDEM1 on the ATF6 activation, observed here, we then sought to determine how this EDEM1 mutant would affect the activation of ATF6 in order to gain some insight into a potential mechanism of ATF6-mediated hepatocellular carcinoma (HCC) development. To test this, HeLa cells were transiently transfected with the FLAG-tagged ATF6 plasmid alone or co-transfected with the wild type (wt) HA-tagged EDEM1 plasmid or the mutant HA-tagged EDEM1-N198I plasmid, then treated or not with DTT (1 mM) for 0.5, 1, 2 and 3 hours. The resulting lysates were immunoblotted with FLAG and EDEM1 antibodies. While overexpression of wt EDEM1 resulted in a kinetics of ATF6 activation similar to that obtained upon overexpression of ATF6 alone but with a smaller activation amplitude, expression of mutant EDEM1 (N198I) led to an early activation of ATF6, with a peak observed after 1 hour of DTT treatment and the reduction of ATF6-p50 at 2-3 hours compared to wt EDEM1 or ATF6 alone (**Figure 5C-D**). Moreover, the comparison of the kinetics of p50-ATF6 appearance upon ER stress in cells expressing EDEM1 wt or N198I revealed that EDEM1 N198I mutant accelerated ATF6 activation upon ER stress (**Figure 5E**). In addition, the normalization of the p50-ATF6 levels with the EDEM1 wt or mutant expression levels did not change the differences in the activation mode of ATF6 (**Figure 5F).** Noteworthy, the N198I mutant exhibited a faster electrophoretic mobility than its corresponding wt form as expected by the nature of the mutation on an N-linked glycosylation site (**Figure 5B-C**). Sequentially, we tested whether this difference in ATF6 activation was due to a change in the physical interaction, if any, between the two proteins. To this end, HeLa cells were transiently co-transfected with the FLAG-tagged ATF6 plasmid and either the wild type or the mutant form of the HA-EDEM1

.

plasmid, then immunoprecipitation for HA tag was performed in the lysates which were immunoblotted using anti-FLAG antibodies. After 2 h of DTT treatment EDEM1 still interacted with the p90-ATF6, and its mutant form also retained the interaction, showing that the alteration in the ATF6 activation is independent of the glycosylation mutation in the EDEM1 (**Figure 5G**). In summary, N198I EDEM1 interacts with ATF6 in the ER as much as the wild-type form does but leads to an accelerated ATF6 cleavage upon ER stress.

EDEM1 expression regulates the stability of full-length ATF6 under basal conditions - Since ATF6 is a natively unstable protein and since EDEM1 contributes to ERAD, we then tested how the expression of wild-type or N198I EDEM1 could impact on ATF6 stability under basal conditions. To do so, we monitored the expression levels of p90-ATF6 throughout a differential overexpression of EDEM1 wild-type or EDEM1-N198I and in a time-course fashion. First, increasing amounts of plasmids coding for EDEM1 wild-type or N198I (0-10 μg) were transfected in HeLa cells and the expression levels of p90-ATF6 was monitored (**Figure 6A**). This revealed the minimal concentration (0.5 μg) of plasmid to transfect to observe an effect of the EDEM1 construct on p90-ATF6 (**Figure 6B**). To further evaluate the impact of wild-type and N198I EDEM1 on ATF6 activation in the absence of ER stress, a cycloheximide pulse experiment was carried out on HeLa cells expressing wild-type or N198I EDEM1 (0.5 μg) (**Figure 6C**), which revealed that N198I EDEM1 induced the sustained activation of ATF6 compared to wild-type EDEM1 (**Figure 6C, D**), and this in the absence of genuine ER stress (not shown). Collectively, these results show that the N198I EDEM1 mutant is able to prompt the sustained activation of ATF6 thereby activating ATF6 adaptive signaling even in the absence of ER stress. The same plasmid concentrations of EDEM1 wt or mutant did not yield any difference in the expression of downstream targets of IRE1 and PERK (*Xbp1s, Gadd34, Chop, Atf4* mRNAs) (**Figure 7).**

EDEM1 N198I expression increases cell resistance to ER stress through ATF6 signaling - In order to validate the hypothesis according to which the expression of N198I EDEM1 could impact on tumor cells resistance to ER stress, we monitored survival, apoptosis and necrosis induction in HeLa and HuH7 cells, the latter being an *in vitro* model of HCC. In addition to the mutant, the silencing of EDEM1 was also tested in HeLa cells to investigate its effect under ER stress conditions. Silenced cells showed a lower resistance to 4 hours of DTT treatment compared to those transfected with the control siRNA (**Figure 8A**), indicating the importance of EDEM1 in the cell survival upon ER stress conditions. Although

.

EDEM1 silencing was found to stabilize ATF6 and favor its activation upon ER stress (**Figure 2**), its absence might also lead to decreased ERAD and consequently increase misfolded proteins accumulation and subsequent proteotoxicity. In addition, both HeLa and HuH7 cells were transiently transfected with either the wild-type or the mutant EDEM1, then treated with DTT (1 mM) or Tun (5 µg/ml) for 8, 24 and 48h, and their survival evaluated. HeLa cells transiently bearing the N198I EDEM1 showed a greater resistance to DTT treatment, whereas HuH7 cells with the same condition appeared with a greater survival under Tun treatment (**Figure 8B-E**). Noteworthy, the overexpression of HA-EDEM1 did not lead to complete rescue of the effect seen with the siEDEM1, but with the mutant N198I the effect was almost completely restored (**Figure 8A-B**). Cells were also treated with Tg following the same procedure as for DDT or Tun. In those conditions, the expression of either the wild type or the N198I EDEM1 forms did not yield any survival advantage (data not shown). This was most likely due to the different ways these chemicals induce ER stress. HeLa and HuH7 transiently expressing either EDEM1 wild-type or N198I EDEM1 were treated with 1 mM DTT and tested for apoptosis/necrosis using FACS analysis and Annexin V/7-AAD staining, respectively. While for both HeLa and Huh7 cells induction of apoptosis was not significantly different between the wild-type and N198I EDEM1 forms (**Figure 9A-C)**, necrosis was significantly altered in HuH7 cells expressing the mutant N198I EDEM1 compared to wild-type EDEM1 (**Figure 8F**). The effect of the mutant EDEM1 was not observed in basal/untreated conditions, result consistent with the absence of ER stress observed in those cells (**Figure 9D)** and the absence of any significant difference between overexpression of wild-type EDEM1 or mutant EDEM1 on the secretion of a cargo protein, alpha-1 antitrypsin (A1AT; **Figure 10A**). Overexpression of wild-type and N198I EDEM1 was confirmed by immunoblot with anti-EDEM1 antibodies (**Figure 8G and 10A**). Then, to address whether the observed advantage given by the mutant EDEM1 was mediated by ATF6, HuH7 cells were silenced for ATF6 concomitantly with the transfection of HA-EDEM1 and HA-EDEM1-N198I plasmids. Under these conditions ATF6 silencing yielded same necrosis levels for both wt and mutant EDEM1 (**Figure 8H**). Efficient silencing of ATF6 was confirmed by qPCR analysis (**Figure 8I**) and was also associated with differential effects on cell survival (**Figure 11**). These results indicate that the EDEM1-dependent ATF6 regulation might contribute to a novel survival pathway involved in cancer development.

Discussion

In this manuscript, we aimed at better characterizing the molecular mechanisms of ATF6 activation and evaluate their contribution to cancer development [23]. First, we confirmed that ATF6 can be degraded by the proteasome in our experimental system and showed that proteasome inhibition under ER stress conditions led to a greater ATF6 activation. We thus

.

raised the hypothesis that this improved activation of ATF6 might result from its stabilization. Subsequently, a siRNA-based screening targeting ER quality control components revealed EDEM1 as a regulator of ATF6 activation. Indeed, EDEM1 silencing led to enhanced ATF6 activation, and consequently greater ATF6 transcriptional activity. EDEM1 is a major player in ERAD of glycoproteins through its weak but consistent α1,2-mannosidase activity [24]. EDEM1 downregulation leads to the stabilization of glycosylated ERAD substrates [25], and is involved in the degradation of ATF6 in non-transformed cells [11]. Our primary siRNA screen also revealed that silencing, EDEM2 or EDEM3, resulted in lower ATF6 Golgi complex and nuclear localisation, a marker of activation. This contrasts with the observed effects of EDEM1 silencing and to the previously reported roles of the other EDEMs in non-transformed cells on ATF6 stability [11] and might suggest cell type-dependent roles of EDEM proteins, however, this observation was not confirmed in a secondary screen.

ATF6 is a glycoprotein with 3 N-linked glycosylation sites at the residues 472, 584 and 643. Based on this, we then evaluated ER stress-mediated activation of ATF6 after kifunensine (KIF) or castanospermine (CST) treatment and we observed that upon α1,2-mannosidase blockade (KIF) ATF6 was further activated, whereas upon glucosidase inhibition (CST) its activation was greatly reduced (**Figure 4A-B**). This revealed the role of ATF6 glycosylation in its activation process. Moreover, stabilization of ATF6 was also dependent on α1,2-mannosidases in the ER and of EDEM1, thereby indicating the role of ATF6 glycosylation on the protein's presence/availability in the ER. Regarding the role of EDEM1 in this process, it is now known that due to inefficient signal sequence cleavage, EDEM1 can be observed either as a membrane-integrated or as a soluble protein [26-28]. This topology has been associated with the protein's specificity to either soluble or membranous substrates: soluble EDEM1 leads to faster degradation of the soluble ERAD substrate (ERAD-Ls) null Hong Kong (NKH) alpha-1 antitrypsin, while transmembrane EDEM1 is more efficient in the turnover of the transmembrane TCRα ERAD substrate (ERAD-Lm) [28]. Based on this, one could propose that the ERAD-Lm substrate ATF6 would be mostly controlled by the low abundance membrane-associated EDEM1.

EDEM1 exhibits 5 potential N-glycosylation sites, at the Asn residues 181, 198, 299, 342, 624. So far, EDEM1 has been observed with either 4 or 5 glucans in its final conformation and the difference lies on the final glycosylation site Asn624 [28]. We recently identified a somatic missense mutation on EDEM1 Asn198 (N198I) in hepatocellular carcinoma (HCC) tumors [15, 16]. Since ATF6 has been associated with HCC development [21, 22], and since its activation was regulated by EDEM1, we reasoned that cancer-associated mutations in EDEM1 might slightly change the protein properties towards ATF6 and therefore promote its adaptive functions, thereby favoring cancer cell growth. Herein, we show that the EDEM1

.

N198I mutant leads to an altered ATF6 activation pattern under ER stress compared to the wt EDEM1 in HeLa cells. More importantly, the mutant conferred ER stress resistance to both HeLa and HuH7 cells (**Figure 8B-E**). Furthermore, HuH7 cells expressing the EDEM1 N198I mutant were more resistant to ER stress-induced necrosis than cells expressing wt EDEM1. This effect was reversed by knocking down ATF6 indicating its involvement in the cancer advantageous effects of EDEM1 N198I (**Figure 8**). However our results do not specify the nature of this EDEM1 somatic mutation. Provided that this mutation is rare, it is likely that it is a passenger mutation that enhances pro-tumorigenic properties through the stabilization of ATF6 and its subsequent enhanced activation.

Co-immunoprecipitation experiments showed that EDEM1 N198I interacts with ATF6 as efficiently as wild-type EDEM1, thus suggesting that additional factors should be involved. A first possibility might be that EDEM1 N198I enzymatic activity could be further reduced thus reducing the entry of ATF6 into ERAD. A second possibility might rely on a reduced association of EDEM1 N198I with SEL1L leading to the subsequent reduced association with ATF6 in a dynamic manner [28]. Interestingly, ATF6, which is the only SEL1L-dependent ERAD-Lm substrate [13], was further activated upon SEL1L silencing. As a result, the fastest activation of ATF6 caused by EDEM1 N198I could be due to an inefficient/slower delivery to the SEL1L-containing complex, thus attenuating the subsequent ATF6 degradation and increasing its availability for transport to the Golgi complex. Remarkably, EDEM1 N624 was reported to be essential for EDEM1 maturation but without effect on the turnover of NHK alpha-1 antitrypsin, however the effect on a membrane ERAD substrate was not tested. Following the same logic, one could postulate the intervention of other ERAD machinery components involved in the observed effect of the mutant EDEM1 or alternatively the impact of altered EDEM1 glycosylation on its availability in the ER. However, this would not be specific to the ATF6 protein but would also include other ERAD-Lm substrates.

Hence, this study reveals the role of EDEM1-mediated regulation of ATF6 activation in transformed/cancer cells. Moreover, an HCC-associated somatic mutation of EDEM1 (N198I) was functionally studied and found to promote ATF6 activation under basal conditions thereby enhancing cell resistance to ER stress most likely through an hormesis-like mechanism. These data might provide an explanatory mechanism for the proposed pro-oncogenic role of ATF6 in primary liver cancers.

.

Materials and Methods

Materials. Mouse monoclonal anti-ATF6 was from BioAcademia. Mouse monoclonal anti-FLAG M2, dithiothreitol (DTT), MG132 (Z-Leu-Leu-H) and thapsigargin (Tg) and cycloheximide (CHX) were obtained from Sigma-Aldrich. Rabbit polyclonal anti-Giantin antibody was from Abcam. Goat polyclonal anti-EDEM1, goat polyclonal anti-Actin and rabbit polyclonal anti-ERK1 antibodies were from Santa Cruz Biotechnologies. Mouse monoclonal anti-HA was obtained from Roche. Rabbit anti-CNX antibody was kindly provided by Dr. John Bergeron (McGill University, Montreal, Qc, Canada). Castanospermine (CST), kifunensine (KIF) and tunicamycin (Tun) were purchased from Calbiochem. Fluorescent-conjugated secondary antibodies were from Molecular Probes (Invitrogen).

Plasmids. Human ATF6 cDNA was amplified from human total cDNA by PCR and cloned into p3xFLAG-CMV7.1 vector within the *HindIII*/*SalI* restriction sites. pCMV-SPORT2-EDEM1-HA was kindly provided by Dr. Ikuo Wada (Fukushima medical University, Fukushima, Japan). pCMV-SPORT2-EDEM1(N198I)-HA was generated by QuickChange® II XL site-directed mutagenesis kit (Stratagene).

Cell Culture and Transfection. HeLa and Huh7 cells were cultured in Dulbecco's modified Eagle's medium (DMEM) supplemented with 10% fetal bovine serum (FBS) and penicillin-streptomycin (100 U/ml and 100 µg/ml, respectively) at 37°C in a 5% CO_2 incubator. HeLa cells stably expressing 3xFLAG-ATF6α (HeLa-ATF6) [10] were maintained in DMEM with 10% FBS containing 200 µg/ml Hygromycin B (Invitrogen). FLAG-tagged ATF6 (FLAG-ATF6), HA-EDEM1 and HA-EDEM1-N198I proteins were transiently transfected in HeLa and HuH7 cells using Lipofectamine and PLUS reagents or Lipofectamine 2000 (Invitrogen) according to the manufacturer's protocols.

RNA interference. Small interfering RNAs (siRNA) were obtained from RNAi Co. and Ambion. Each siRNA (25 nM) was transfected into HeLa, HeLa-ATF6 or HuH7 cells by reverse transfection using Lipofectamine RNAiMAX (Invitrogen). The sequences of siRNA used in this study are described in **Table S1**.

Immunoblot and immunoprecipitation. Whole cell extracts were prepared using either RIPA buffer (25 mM Tris-HCl pH 7.5, 150 mM NaCl, 1% NP-40, 1% sodium deoxycholate and 0.1% SDS) or SDS sample buffer (50 mM Tris-HCl pH 6.8, 2% SDS, 10% glycerol) after washing cells with ice-cold PBS. To prepare the lysates for the detection of ATF6 using a mouse monoclonal anti-ATF6, cells were lysed in SDS-sample, mixed vigorously and boiled for 5 min. To prepare the extracts for other proteins, the cells were incubated in RIPA buffer for 30 min on ice and cell lysates were centrifuged at 4°C for 20 min at 13,000 rpm. The

.

samples were applied to SDS-PAGE and analyzed by immunoblotting. Dilutions of primary antibodies used for immunoblotting were as follows: mouse monoclonal anti-ATF6, 1:1,000; rabbit polyclonal anti-CNX, 1:2,000; goat polyclonal anti-EDEM1, goat polyclonal anti-Actin, 1:1,000; rabbit polyclonal anti-ERK, 1:1,000; mouse monoclonal anti-FLAG M2, 1:2,000; mouse monoclonal anti-HA, 1:1,000. For the immunoprecipitation analysis, the cells were lysed in CHAPS buffer (30mM Tris-HCl pH7.5, 150mM NaCl and 1.5% CHAPS) and then incubated 16 h at 4°C with the HA antibody (1µg Ab/1000µg protein). After this, dynabeads protein G (Life Technologies) were first washed with CHAPS lysis buffer and/or PBS, then mixed with the protein/Ab mixture, incubated at room temperature for 20 min with gentle rotation and washed with CHAPS and/or PBS. Finally, the beads were eluted with 1x Laemmli sample buffer, heated at 55°C for 5 min and loaded to SDS-PAGE. For the immunoblotting anti-FLAG M2 was used as described before.

Indirect immunofluorescence. HeLa cells transiently expressing FLAG-ATF6 were cultured on coverslips in 24-well plate and fixed in methanol at -20°C for 5 min. Then, cells were blocked in immunofluorescence buffer (0.15 M NaCl, 2 mM EGTA, 1 mM $MgCl_2$ and 10 mM PIPES-Na pH 7.2) containing 3% bovine serum albumin (BSA) for 30 min and incubated with primary (anti-FLAG M2, 1:500; anti-CNX, 1:500 or anti-Giantin, 1:1,000) and secondary (Alexa-488 labelled anti-mouse IgG or Alexa-568 labelled anti-rabbit IgG, 1:250, respectively) antibodies for 1 h at room temperature. Nuclei were stained using Hoechst 33342 (Invitrogen). Coverslips were mounted on microscope slides using Fluoromount-G (SouthernBiotech) and observed using a Leica TCS SP5 confocal microscope with 63x oil immersion objective.

Quantitative RT-PCR (q-PCR). Total RNA was extracted from 48 h after siRNA- transfected cells using TRIZOL reagent (Invitrogen) according to the manufacturer's instruction. cDNA was synthesized from the total RNA using SuperScript First-Strand Synthesis System (Invitrogen) or Reverse Transcription System (Promega) with Oligo(dT) primer (Invitrogen). cDNA was analyzed with B-R SYBR Green SuperMix (Quanta Bioscience) in StepOnePlus™ system (Applied Biosystems). The primer sequences used for this experiment are shown in **Table S2.**

^{35}S-methionine pulse-chase experiments. Expression of EDEM1 in HeLa-ATF6 was silenced by 25 nM of siRNA for 72 h. Cells were then incubated in methionine- and cysteine-free DMEM with 10% DMEM for 2 h. KIF (5 µg/ml) was added to HeLa-ATF6 cells 2 h prior to starvation. Cells were pulse-labelled with 100 mCi/60 mm dish of EXPRE^{35}S^{35}S Protein Labelling Mix (PerkinElmer) for 30 min. Labelled cells were washed twice with ice-cold PBS and chased in complete medium (DMEM containing 10% FBS) for 0 to 4 h. Pulse labelling

.

and chase were also carried out in the presence and absence of KIF. Pulse-labelled cells were washed twice with PBS and incubated in Lysis buffer (30 mM Tris-HCl pH 7.5, 150 mM NaCl and 1% Triton X-100) for 30 min on ice and centrifuged at 13,000 rpm for 20 min at 4°C. After pre-clearing using protein G Sepharose (GE Healthcare Bio-Sciences), lysates were incubated overnight with anti-FLAG antibody (1:200) at 4°C. The beads were then added to the immune complexes and precipitated for 1 h at 4°C with gentle rotation and washed five times with Lysis buffer. Immunoprecipitates were eluted with Laemmli sample buffer containing 50 mM DTT for 10 min at 70°C. The proteins were analyzed by immunoblotting and detected using LumiGLO chemiluminescent substrate system (Kirkegaard & Perry Laboratories).

Toxicity and necrosis/apoptosis assays. HeLa and HuH7 cells were transiently transfected with either HA-EDEM1 or HA-EDEM1-N198I. Twenty-four hours later the cells were re-plated in 96-well plates, where they were left untreated or treated with 1mM DTT or 5µg/ml Tun for 8, 24 and 48 h. The WST1 reagent was added in a 1:10 ratio to the wells of the plates for the different time-points when appropriate. The plates were incubated for 4 h at 37°C and then the absorbance was measured in a plate reader at 450nm and 600nm, with the final measurement being the subtraction of the two values. To determine the extent of cell death, HeLa and HuH7 cells were transiently transfected with either HA-EDEM1 or HA-EDEM1-N198I. Twenty-four hours later the medium was changed and 1mM DTT was added to the cells for 0, 4 and 8 h. At the end of the time course, the cells were collected in glass tubes, along with the corresponding supernatants and PBS washes, and centrifuged at 1,700 rpm or 750 x g for 7 min. 1x Annexin V buffer and Annexin V were added to the cell pellets that were incubated at RT for 15 min, then 2% FCS in PBS and 7-AAD were added to the samples which were incubated at RT for 5-10 min before analyzing them by flow cytometry in a BD FACSCanto II.

Statistical analyses. Statistical analysis was performed using the GraphPad Prism 7.0a software using the student's t-test.

Acknowledgements

We thank Pr. Jessica Zucman-Rossi (Inserm, France) for help with HCC variant analyses and Dr Maurizio Molinari (IRB, Switzerland) for discussions. This work was supported by grants from Institut National du Cancer (INCa_5869, INCa_7981, INCa_PLBIO_ 2015-111; ICGC; INCa_PLBIO_2017), EU H2020 MSCA ITN-675448 (TRAINERS) and MSCA RISE-

.

734749 (INSPIRED) and La Fondation pour la Recherche Médicale (FRM, équipe labellisée 2018).

Conflict of Interest

The authors declare that they have no conflict of interest regarding this study.

Author Contributions

AH and AP designed and conducted experiments and analyzed the data. TA, LS, OP and GJ conducted some of the experiments, RP and FJ carried out animal experiments. OP and EC supervised the whole work. All the authors worked on the manuscript.

References

1. Hetz, C., Chevet, E. & Oakes, S. A. (2015) Proteostasis control by the unfolded protein response, *Nat Cell Biol.* **17**, 829-38.

2. Harding, H. P., Zhang, Y. & Ron, D. (1999) Protein translation and folding are coupled by an endoplasmic-reticulum-resident kinase, *Nature.* **397**, 271-4.

3. Lu, Y., Liang, F. X. & Wang, X. (2014) A synthetic biology approach identifies the mammalian UPR RNA ligase RtcB, *Mol Cell.* **55**, 758-70.

4. Tanaka, N., Meineke, B. & Shuman, S. (2011) RtcB , a Novel RNA Ligase , Can Catalyze tRNA Splicing and HAC1 mRNA Splicing in Vivo * □. **286**, 30253-30257.

5. Yoshida, H., Matsui, T., Yamamoto, A., Okada, T. & Mori, K. (2001) XBP1 mRNA is induced by ATF6 and spliced by IRE1 in response to ER stress to produce a highly active transcription factor, *Cell.* **107**, 881-91.

6. Maurel, M., Chevet, E., Tavernier, J. & Gerlo, S. (2014) Getting RIDD of RNA: IRE1 in cell fate regulation, *Trends Biochem Sci.* **39**, 245-254.

7. Urano, F., Wang, X., Bertolotti, A., Zhang, Y., Chung, P., Harding, H. P. & Ron, D. (2000) Coupling of stress in the ER to activation of JNK protein kinases by transmembrane protein kinase IRE1, *Science.* **287**, 664-6.

8. Haze, K., Yoshida, H., Yanagi, H., Yura, T. & Mori, K. (1999) Mammalian transcription factor ATF6 is synthesized as a transmembrane protein and activated by proteolysis in response to endoplasmic reticulum stress, *Mol Biol Cell.* **10**, 3787-99.

.

9. Nadanaka, S., Okada, T., Yoshida, H. & Mori, K. (2007) Role of disulfide bridges formed in the luminal domain of ATF6 in sensing endoplasmic reticulum stress, *Mol Cell Biol.* **27**, 1027-43.

10. Higa, A., Taouji, S., Lhomond, S., Jensen, D., Fernandez-Zapico, M. E., Simpson, J. C., Pasquet, J. M., Schekman, R. & Chevet, E. (2014) Endoplasmic reticulum stress-activated transcription factor ATF6alpha requires the disulfide isomerase PDIA5 to modulate chemoresistance, *Mol Cell Biol.* **34**, 1839-49.

11. Ninagawa, S., Okada, T., Sumitomo, Y., Horimoto, S., Sugimoto, T., Ishikawa, T., Takeda, S., Yamamoto, T., Suzuki, T., Kamiya, Y., Kato, K. & Mori, K. (2015) Forcible destruction of severely misfolded mammalian glycoproteins by the non-glycoprotein ERAD pathway, *J Cell Biol.* **211**, 775-84.

12. Hong, M., Li, M., Mao, C. & Lee, A. S. (2004) Endoplasmic reticulum stress triggers an acute proteasome-dependent degradation of ATF6, *J Cell Biochem.* **92**, 723-32.

13. Horimoto, S., Ninagawa, S., Okada, T., Koba, H., Sugimoto, T., Kamiya, Y., Kato, K., Takeda, S. & Mori, K. (2013) The unfolded protein response transducer ATF6 represents a novel transmembrane-type endoplasmic reticulum-associated degradation substrate requiring both mannose trimming and SEL1L protein, *J Biol Chem.* **288**, 31517-27.

14. Chevet, E., Cameron, P. H., Pelletier, M. F., Thomas, D. Y. & Bergeron, J. J. (2001) The endoplasmic reticulum: integration of protein folding, quality control, signaling and degradation, *Curr Opin Struct Biol.* **11**, 120-4.

15. Guichard, C., Amaddeo, G., Imbeaud, S., Ladeiro, Y., Pelletier, L., Maad, I. B., Calderaro, J., Bioulac-Sage, P., Letexier, M., Degos, F., Clement, B., Balabaud, C., Chevet, E., Laurent, A., Couchy, G., Letouze, E., Calvo, F. & Zucman-Rossi, J. (2012) Integrated analysis of somatic mutations and focal copy-number changes identifies key genes and pathways in hepatocellular carcinoma, *Nat Genet.* **44**, 694-8.

16. Schulze K, Imbeaud S, Letouzé E, Alexandrov LB, Calderaro J, Rebouissou S, Couchy G, Meiller C, Shinde J, Soysouvanh F, Calatayud AL, Pinyol R, Pelletier L, Balabaud C, Laurent A, Blanc JF, Mazzaferro V, Calvo F, Villanueva A, Nault JC, Bioulac-Sage P, Stratton MR, Llovet JM, Zucman-Rossi J. (2015) Exome sequencing of hepatocellular carcinomas identifies new mutational signatures and potential therapeutic targets. *Nat Genet.* **47**, 505-511.

17. Hong, M., Luo, S., Baumeister, P., Huang, J. M., Gogia, R. K., Li, M. & Lee, A. S. (2004) Underglycosylation of ATF6 as a novel sensing mechanism for activation of the unfolded protein response, *J Biol Chem.* **279**, 11354-63.

18. Nadanaka, S., Yoshida, H. & Mori, K. (2006) Reduction of disulfide bridges in the lumenal domain of ATF6 in response to glucose starvation, *Cell Struct Funct.* **31**, 127-34.

19. Adachi, Y., Yamamoto, K., Okada, T., Yoshida, H., Harada, A. & Mori, K. (2008) ATF6 is a transcription factor specializing in the regulation of quality control proteins in the endoplasmic reticulum, *Cell Struct Funct.* **33**, 75-89.

20. Yamamoto, K., Sato, T., Matsui, T., Sato, M., Okada, T., Yoshida, H., Harada, A. & Mori, K. (2007) Transcriptional induction of mammalian ER quality control proteins is mediated by single or combined action of ATF6alpha and XBP1, *Dev Cell.* **13**, 365-76.

21. Arai, M., Kondoh, N., Imazeki, N., Hada, A., Hatsuse, K., Kimura, F., Matsubara, O., Mori, K., Wakatsuki, T. & Yamamoto, M. (2006) Transformation-associated gene regulation by ATF6alpha during hepatocarcinogenesis, *FEBS Lett.* **580**, 184-90.

.

22. Shuda, M., Kondoh, N., Imazeki, N., Tanaka, K., Okada, T., Mori, K., Hada, A., Arai, M., Wakatsuki, T., Matsubara, O., Yamamoto, N. & Yamamoto, M. (2003) Activation of the ATF6, XBP1 and grp78 genes in human hepatocellular carcinoma: a possible involvement of the ER stress pathway in hepatocarcinogenesis, *J Hepatol.* **38**, 605-14.

23. Chevet, E., Hetz, C. & Samali, A. (2015) Endoplasmic Reticulum Stress-Activated Cell Reprogramming in Oncogenesis, *Cancer Discov.* **5**, 586-597.

24. Olivari, S., Cali, T., Salo, K. E., Paganetti, P., Ruddock, L. W. & Molinari, M. (2006) EDEM1 regulates ER-associated degradation by accelerating de-mannosylation of folding-defective polypeptides and by inhibiting their covalent aggregation, *Biochem Biophys Res Commun.* **349**, 1278-84.

25. Molinari, M., Calanca, V., Galli, C., Lucca, P. & Paganetti, P. (2003) Role of EDEM in the release of misfolded glycoproteins from the calnexin cycle, *Science.* **299**, 1397-400.

26. Hosokawa, N., Wada, I., Hasegawa, K., Yorihuzi, T., Tremblay, L. O., Herscovics, A. & Nagata, K. (2001) A novel ER alpha-mannosidase-like protein accelerates ER-associated degradation, *EMBO Rep.* **2**, 415-22.

27. Olivari, S., Galli, C., Alanen, H., Ruddock, L. & Molinari, M. (2005) A novel stress-induced EDEM variant regulating endoplasmic reticulum-associated glycoprotein degradation, *J Biol Chem.* **280**, 2424-8.

28. Tamura, T., Cormier, J. H. & Hebert, D. N. (2011) Characterization of early EDEM1 protein maturation events and their functional implications, *J Biol Chem.* **286**, 24906-15.

.

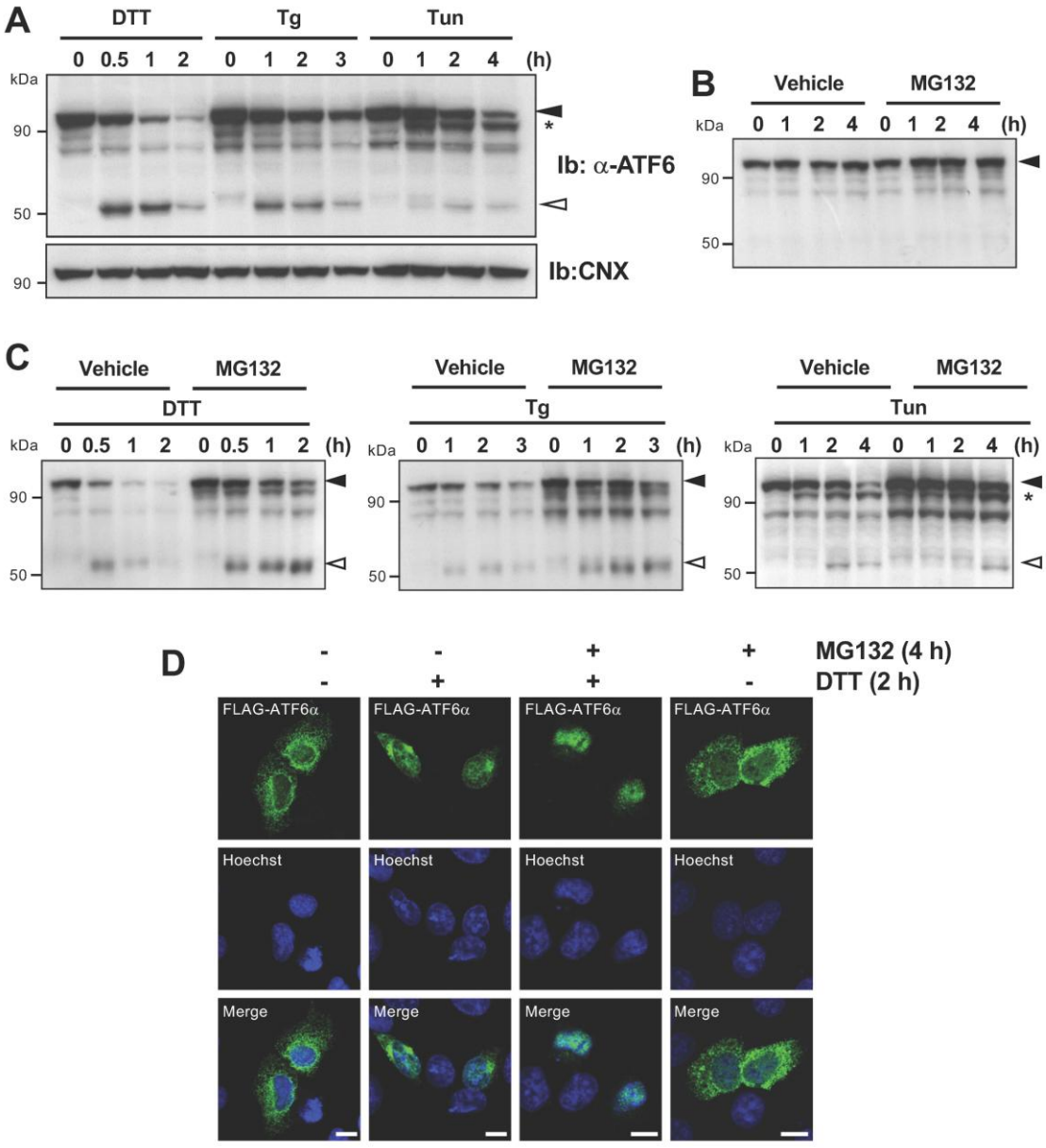

Figure 1. Export of ATF6 from the ER upon ER stress (**A**) HeLa cells were treated with 1 mM DTT, 500 nM Tg or 5 μg/ml Tun for the indicated periods. Whole cell extracts were immunoblotted with anti-ATF6 antibody. Full length and cleaved form of ATF6 are indicated as black and white arrowheads, respectively. The asterisk shows the non-glycosylated form of ATF6. (**B**) HeLa cells were either treated with DMSO (vehicle) or 10 mM MG132 for the indicated periods of time or (**C**) for 4 h prior to treatment of 1 mM DTT, 500 nM Tg or 5 μg/ml Tun for the indicated periods of time. Cell lysates were analyzed by immunoblotting using anti-ATF6 antibody. Full length and cleaved form of ATF6 are indicated as black and white arrowheads, respectively. (**D**) HeLa cells were transfected with FLAG-ATF6. Twenty-four hours after transfection, cells were either treated with DMSO or 10 mM MG132 for 4 h prior to treatment of 1 mM DTT for 2 h. Cells were then immunostained with anti-FLAG for ATF6 and stained with Hoechst 33342 for nuclei. Cells were analyzed by confocal microscope. Bars, 10 μm.

.

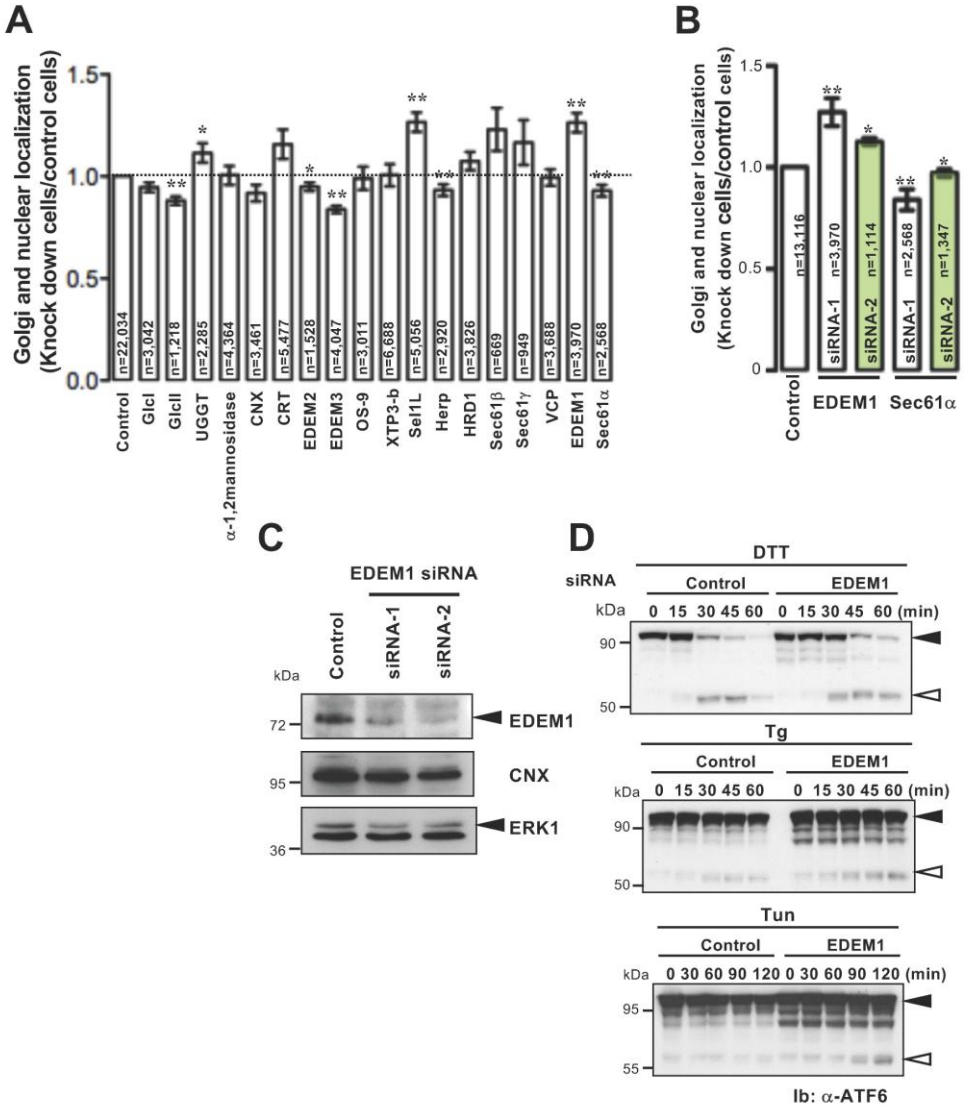

Figure 2. EDEM1 as a regulator of ATF6 activation upon ER stress (**A**) siRNA screen in HeLa cells. HeLa cells were transfected with siRNA (25 nM) and 24 h after cells were further transfected with FLAG-ATF6. Following transfections, cells were treated with 1 mM DTT for 2 h and co-stained with antibodies against FLAG and CNX or Giantin. The number of cells with Golgi apparatus and nuclear staining was counted using confocal microscope. The percentage of Golgi apparatus and nuclear localization in siRNA-transfected cells was calculated and compared with that in control siRNA-transfected cells. Data represented are the mean ±SD of triplicate experiments (*p<0.05 and **p<0.01, as compared to control). (n), number of cells counted for each siRNA experiment. (**B**) The siRNA screen described in (A) plus a validation screen, conducted the same way as the primary screen, for the ERQC components having a consistent effect: EDEM1 and Sec61α. The two screens are denoted with different colours. siRNA-1 and siRNA-2 (green) were respectively used for the primary and validation screens. The analysis for ATF6 export from the ER was done by cell counting as in (A). (n), number of cells counted for each siRNA experiment. Data represented are the average ±SD of triplicate experiments (*p<0.05 and **p<0.01, as compared with control). (**C**) HeLa cells were transfected with control or two each EDEM1 siRNA. Cell lysates were prepared from 48 h post transfection cells and immunoblotted with anti-EDEM1 antibody. Anti-CNX and anti-ERK1 antibodies were used as loading controls. (**D**) siRNAs against EDEM1 were transfected into HeLa-ATF6□cells. Seventy-two hours after siRNA transfection, cells were treated with 1 mM DTT, 500 nM Tg or 5 μg/ml Tun for the indicated time. Cell lysates were analyzed by immunoblotting using anti-ATF6 antibody.

.

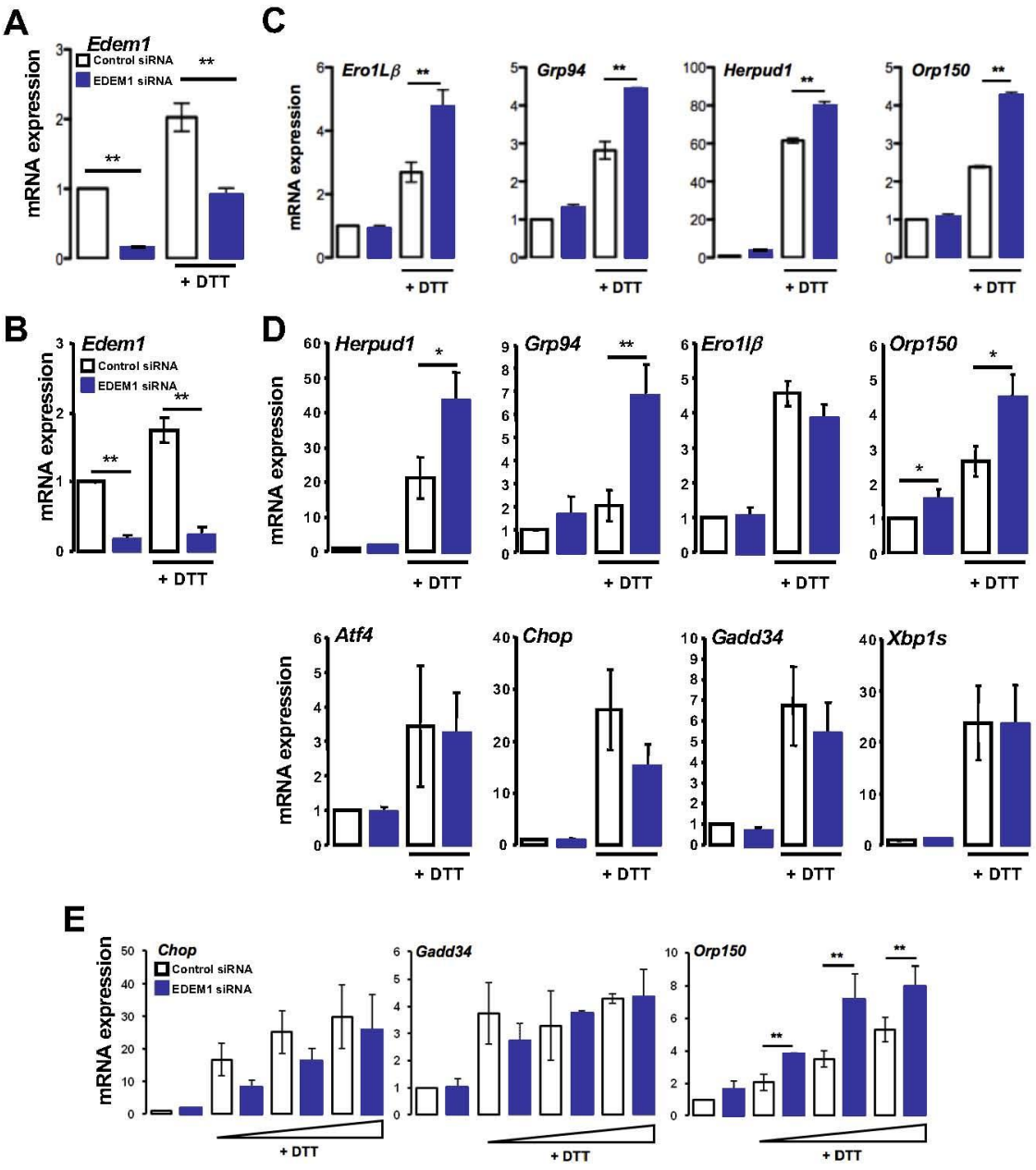

Figure 3. Effects of EDEM1 silencing on ATF6 target genes. (**A-B**) Quantitative RT-PCR (q-PCR) analysis of *Edem1* mRNA expression following siRNA transfection (for 48 h) in HeLa cells (A) and NHDFs (B). Normalization was carried out with *Gapdh*. Data is shown as the average of three independent experiments ±SD (**p<0.01, as compared with control). (**C**) EDEM1 was silenced by siRNA (25 nM) in HeLa cells, 48 h later cells were treated with 1 mM DTT for 2 h. Total RNA was isolated and analyzed by q-PCR using specific primers for ATF6 target genes (*Ero1Lb*, *Grp94*, *Herpud1* and *Orp150*). Each mRNA expression was normalized to *Gapdh* mRNA. Data is shown as the average of three independent experiments ±SEM (**p < 0.01, as compared with control upon DTT treatment). (**D**) EDEM1 was silenced by siRNA (25 nM) in NHDFs, 48 h later cells were treated with 1 mM DTT for 2 h. Total RNA was isolated and analyzed by q-PCR using specific primers for ATF6 target genes and UPR target genes (*Atf4, Chop, Gadd34* and *Xbp1s*). Each mRNA expression was normalized to *Gapdh* mRNA. Data is shown as the average of three independent experiments ±SEM (*p < 0.05 and **p < 0.01, as compared with control upon DTT treatment). (**E**) NHDFs were silenced for EDEM1 using siRNA (25nM) and 48h later, cells were treated or not with increasing DTT concentrations. Total RNA was isolated and analysed by q-PCR using specific primers for *Chop, Gadd34* and *Orp150*. Each mRNA expression was normalized to *Gapdh* mRNA. Data is shown as the average of three independent experiments ±SEM (**p < 0.01, as compared with control upon DTT treatment).

.

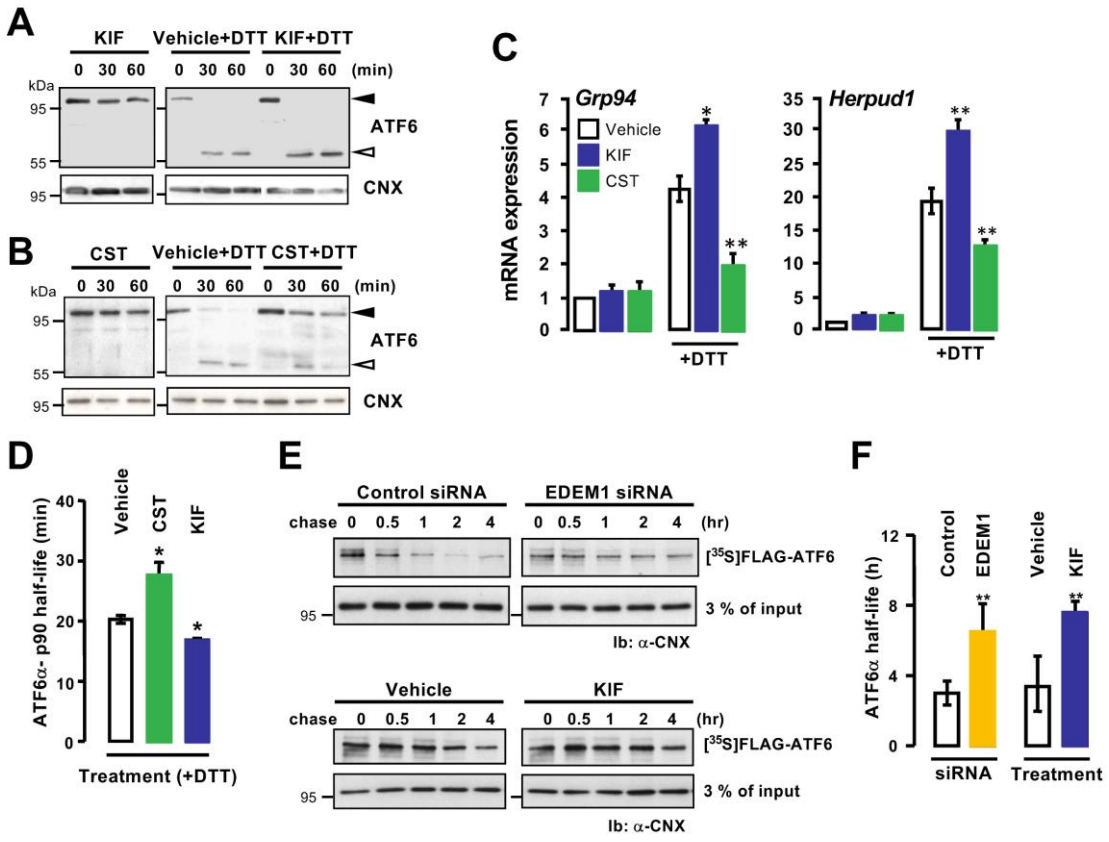

Figure 4. Role of EDEM1 in ATF6 stability. (**A-B**) Immunoblot analysis of ATF6 cleavage upon DTT treatment in the presence or not of 5 µg/ml KIF (A) or of 1 mM CST (B). (**C**) Half-life of ATF6-p90 in cells untreated or treated with KIF or CST under stressed conditions. The experiments were carried out using a 15 min ^{35}S-Met pulse and a chase over 5 h followed immmunoprecipitation with anti-FLAG antibodies. Immunoprecipitates were resolved by SDS-PAGE and the gels exposed to X-Ray films. (**D**) ATF6 target genes, *Grp94* and *Herpud1* mRNA expression upon DTT treatment or not in the presence or not of KIF or CST. (**E**) Half-life of ATF6-p90 in cells silenced for EDEM1 or in cells treated with KIF. The amount of ATF6-p90 was determined using immunoblotting with anti-FLAG antibodies (different exposures were used for revealing the X-Ray films in the two separate experiments: top and bottom panel). (**F**) Quantification of (E).

.

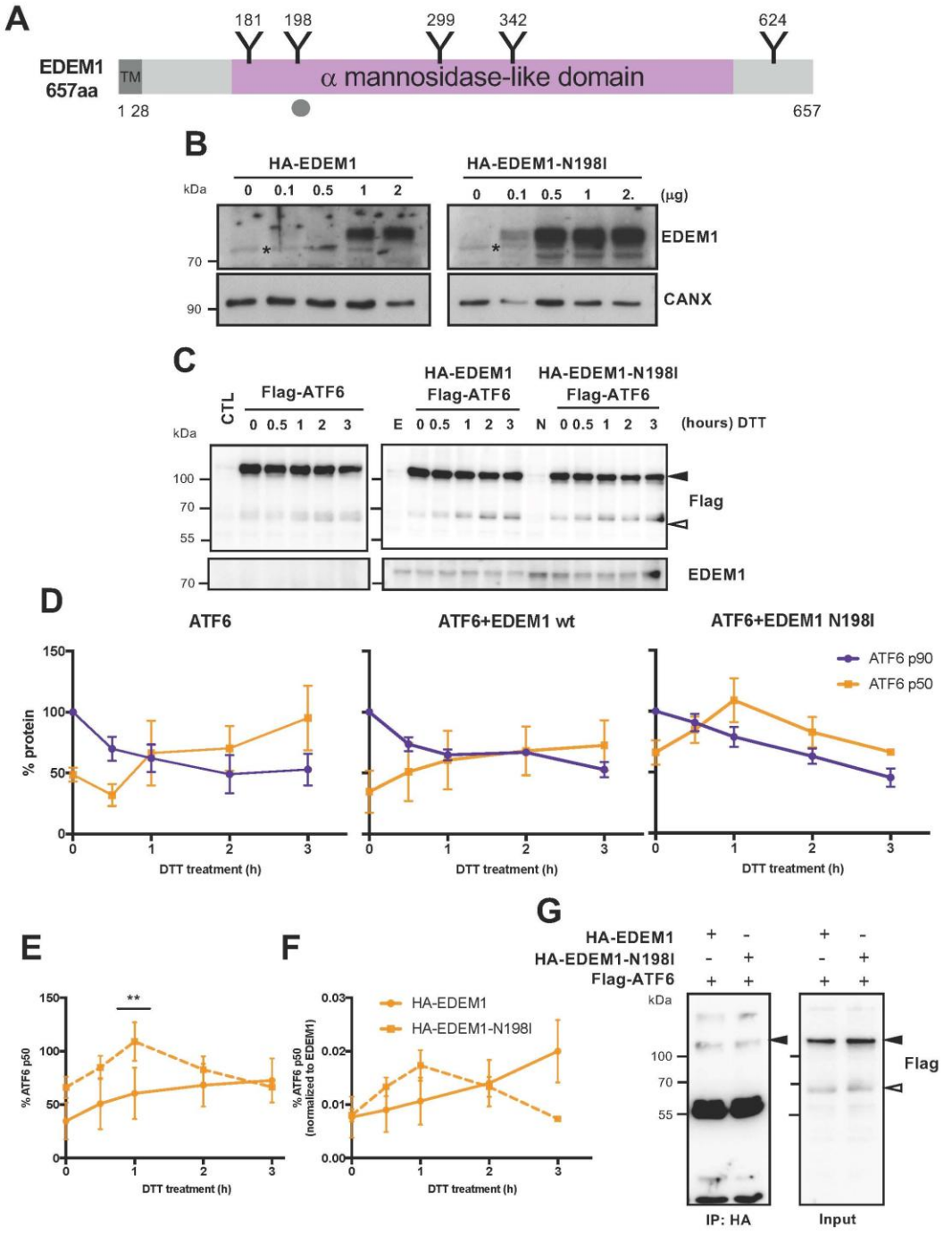

Figure 5. Comparison of the impact of EDEM1 wild type and N198I mutant on ATF6 activation. (**A**) Schematic representation of the EDEM1 protein and its N-linked glycosylation sites. (**B**) Expression of 0.1, 0.5, 1 and 2 µg of the HA-EDEM1 and HA-EDEM1-N198I plasmids in HeLa cells. (**C**) HeLa cells were transfected with FLAG-ATF6 plasmid alone (0.5µg) or along with (0.25µg) HA-EDEM1 (0.5µg) or HA-EDEM1-N198I (0.5µg). 24 hours later the cells were treated with 1mM DTT for 0, 0.5, 1, 2 and 3 hours and then lysed in RIPA buffer. The protein lysates were immunoblotted for FLAG and EDEM1. The western blot shown here is representative of three independent experiments. (**D**) Protein quantification using the ImageJ software for the experiment described in (C) with 100% being the ATF6-p90 protein level at 0h time-point in each case. (**E**) Protein quantification as in (D) for ATF6-p50 only from cells co-expressing FLAG-ATF6 with HA-EDEM1 or HA-EDEM1-N198I. The data are representative of three or more independent experiments and the values shown are the mean ±SEM of the respective experiments (**p<0.01) (**F**) Protein quantification of ATF6-p50 from Figure 5E normalized to the HA-EDEM1 or HA-EDEM1-N198I expression levels (data are representative of three or more independent experiments and the values shown are the mean ±SEM of the respective experiments). (**G**) HeLa cells were transfected with FLAG-ATF6 (0.25µg) and HA-EDEM1 (0.5µg) or HA-EDEM1-N198I (0.5µg). After 24 hours, cells were treated with 1mM DTT for 2 hours followed by immunoprecipitation using the HA antibody. The resultant immunoprecipitates along with the respective input samples were applied to SDS-PAGE and immunoblotted for FLAG. CTL: Control/untransfected; E: HA-EDEM1; N: HA-EDEM1-N198I.

.

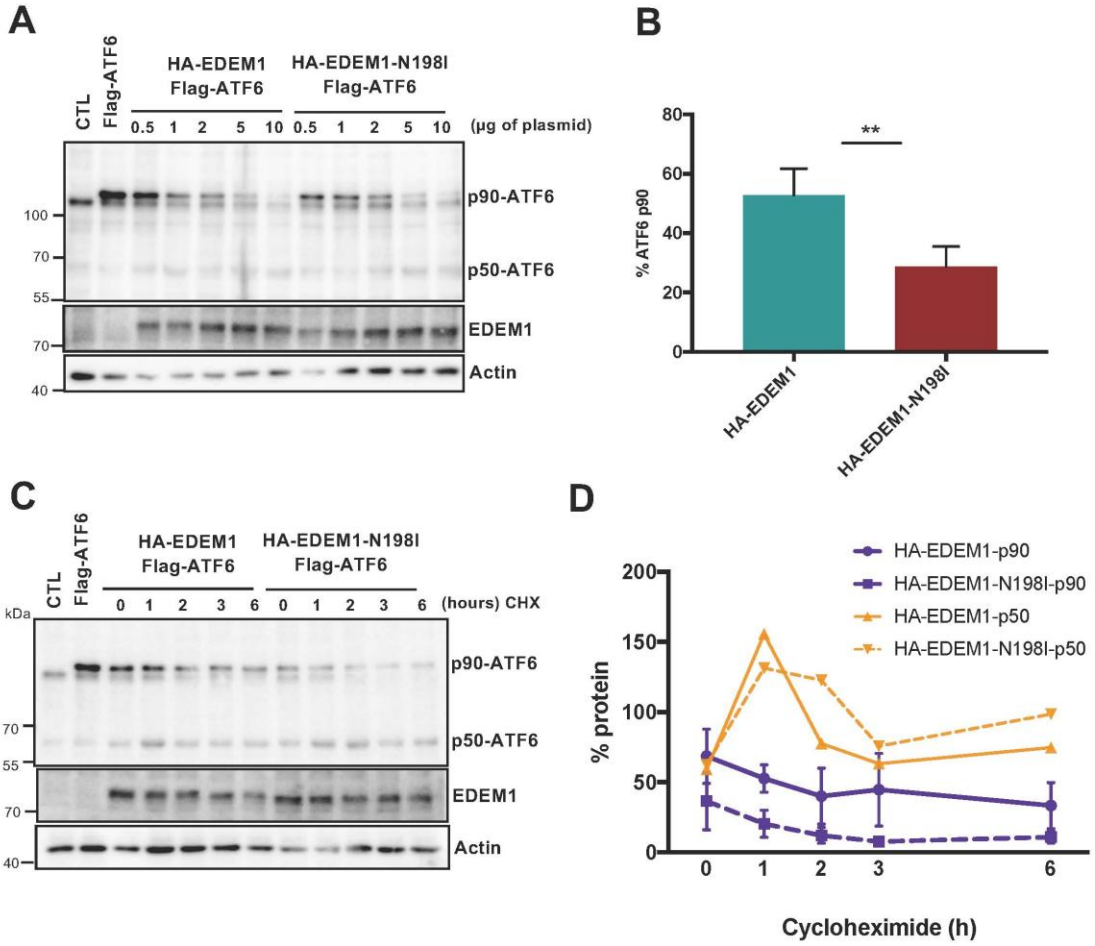

Figure 6. The differential effect of EDEM1 wild type and N198I mutant on the full-length ATF6 protein under unstressed conditions. (**A**) HeLa cells were transfected with FLAG-ATF6 plasmid (0.5μg) alone or in combination with HA-EDEM1 or HA-EDEM1-N198I plasmids at a series of different doses: 0.5, 1, 2, 5, and 10μg. The cells were lysed 24 hours post-transfection in RIPA buffer. Equal amounts of protein lysates were immunoblotted for ATF6, EDEM1 and Actin. (**B**) Protein quantification of the experiment described in (A) for the ATF6-p90 form. A statistical difference between the two EDEM1 forms was shown only for the dose of 0.5μg, represented in the bar graph here. The ATF6-p90 protein level at the "Flag-ATF6" alone condition is regarded as 100%. (**C**) HeLa cells were transfected with FLAG-ATF6 plasmid (0.5μg) alone or in combination with HA-EDEM1 or HA-EDEM1-N198I plasmids (0.5μg). 24 hours later, the cells were either left untreated (0h time-point) or treated with cycloheximide (CHX) at a final concentration of 5μg/ml for 1, 2, 3, and 6 hours. Equal amounts of protein lysates were immunoblotted for ATF6, EDEM1 and Actin. (**D**) Quantification of the results presented in (C) for the ATF6-p90 form with 100% being the ATF6-p90 protein level of the "Flag-ATF6" alone condition. Western blots shown in (A) and (C) and the resulting data shown in (B) and (D) are representative of three or more independent experiments. Data values are the mean ±SEM of the respective experiments (**p<0.01).

.

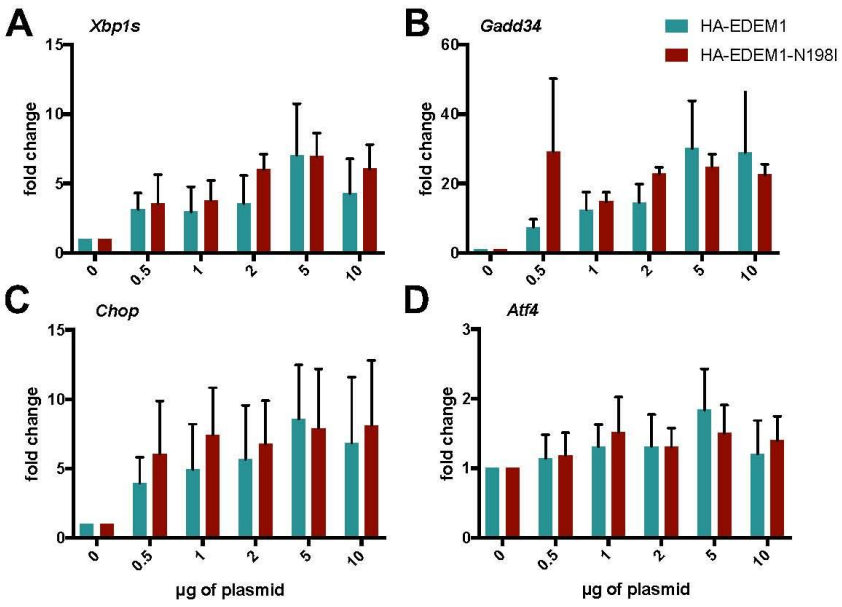

Figure 7. Impact of HA-EDEM1 wt and N198I variant on UPR activation. HeLa cells were transfected with HA-EDEM1 or HA-EDEM1-N198I plasmids at a series of different doses: 0.5, 1, 2, 5, and 10µg. The cells were collected 24 hours post-transfection in TRIZOL. RNA extraction and reverse transcription followed and the resulting cDNA samples were analyzed by qPCR for *Xbp1s, Gadd34, Chop* and *Atf4* mRNA levels. Data are representative of three independent experiments and the values shown are the mean ±SEM of the respective experiments.

.

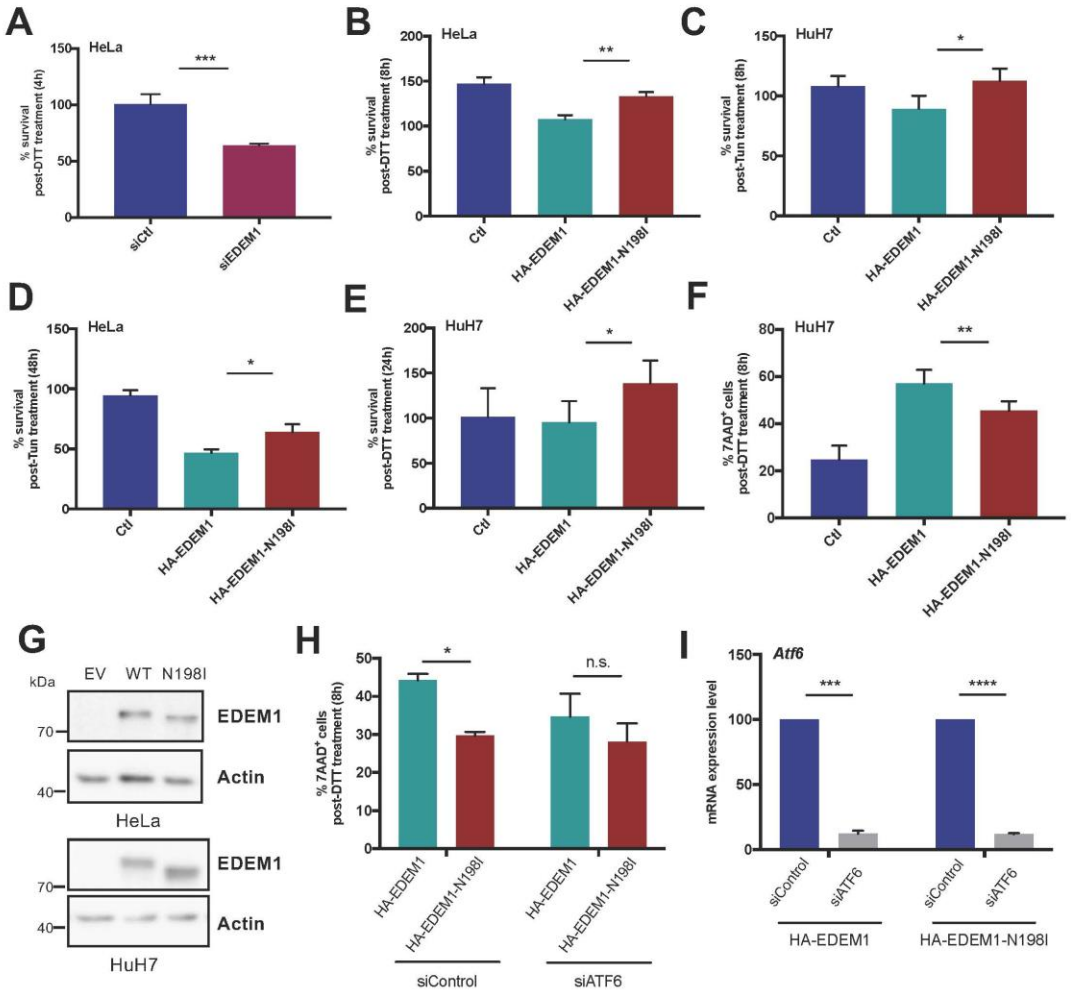

Figure 8. EDEM1 N198I enhances cell resistance to ER stress through ATF6-dependent mechanisms. (**A**) HeLa cells were silenced for EDEM1 using siRNA for 48 hours, and then treated with 1mM DTT for 4 hours. The survival of the cells was assessed by SRB assay and measured at an absorbance of 570nm. (**B, D**) HeLa cells were transfected with HA-EDEM1 (1µg) or HA-EDEM1-N198I (1µg), and then left untreated or treated with 1mM DTT or 5µg/ml Tun for 8, 24 and 48 hours. Cell survival was measured using the WST1 assay. The bars indicated are normalised to the 0h time-point or to the "non-treated cells" wells in the 96-well plates of the assay, which is expressed as 100% absorbance. Data for 8h and 48h are presented. (**C, E**) HuH7 cells were treated like the HeLa cells in (B, D). Data for 8h and 24h are shown. (**F**) HuH7 cells were transfected with HA-EDEM1 (1µg) or HA-EDEM1-N198I (1µg) for 24 hours, and then treated with 1mM DTT for 8 hours. The cells were stained with Annexin V and 7-AAD and assessed using flow cytometry. (**G**) EDEM1 blot under the conditions described in (B-E). (**H**) HuH7 cells were transfected with siATF6 (25 nM) for 48 hours and HA-EDEM1 (1µg) or HA-EDEM1-N198I (1µg) for 24 hours, and then cells were treated as in (F). (**I**) ATF6 qPCR, after normalization to GAPDH mRNA expression levels. Data shown in (A-F) and in (H) are representative of three or more independent experiments and the values shown are the mean ±SEM of the respective experiments (*p<0.05, **p<0.01, ***p<0.001), while data shown for (I) are representative of three technical replicates and the values shown are the mean ±SD of the respective experiments (***p<0.001 and ****p<0.0001). Ctl: Control/untransfected; EV: empty vector.

.

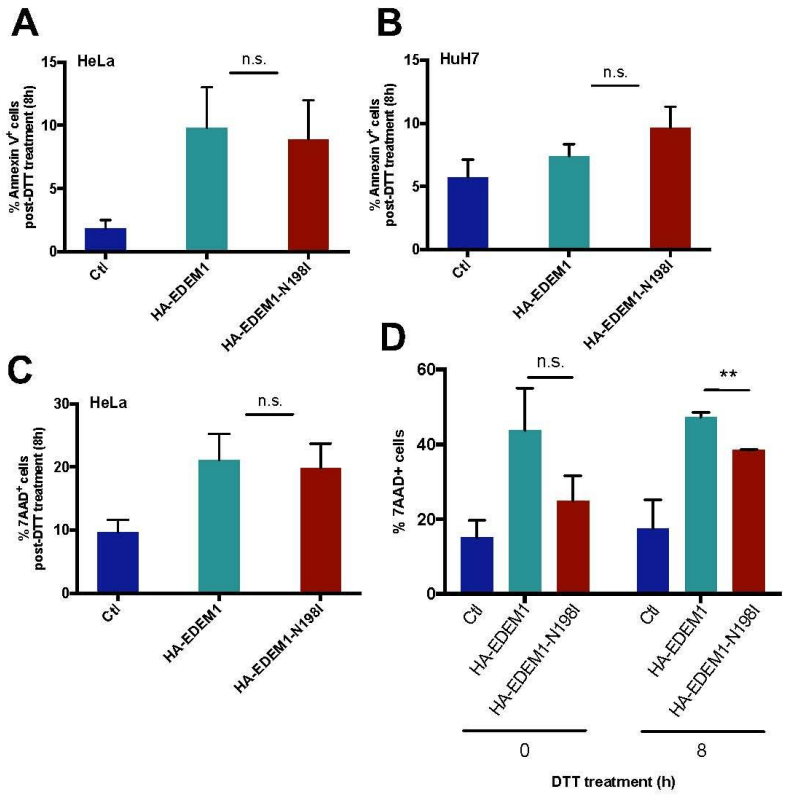

Figure 9. Evaluation of the impact of wt or N198I EDEM1 expression on cell sensitivity to stress. (**A-D**) HeLa and HuH7 cells were transfected with HA-EDEM1 (1µg) or HA-EDEM1-N198I (1µg), and then treated with 1mM DTT for 0, 4 and 8 hours. The cells were stained with Annexin V and 7-AAD and assessed with flow cytometry. The 8h time-point is shown for % Annexin V^+ HeLa (A) and HuH7 (B) cells, and for % $7AAD^+$ HeLa cells (C), or HuH7 cells (D). The bars are representative of three independent experiments and the values shown are the mean ±SEM of the respective experiments (n.s.: non-significant). Ctl: Control/untransfected.

.

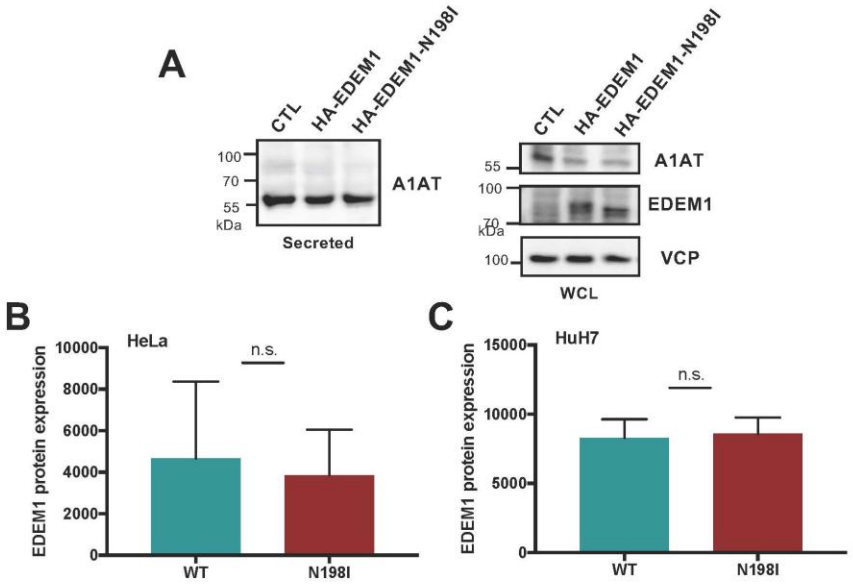

Figure 10. EDEM1 wt and N198I impact on protein secretion and expression quantification. (A) HuH7 cells were transfected with HA-EDEM1 (1µg) or HA-EDEM1-N198I (1µg) in reduced serum media (Opti-MEM). After 24 hours the supernatants were

.

collected and the proteins contained were precipitated with ice-cold acetone over-night. After centrifugation and removal of the supernatant the resulting pellets were resuspended in 1x LSB. At the same time whole cell lysates (WCL) were kept by lysing the cells in RIPA buffer. The samples of the secreted proteins along with their corresponding WCL were immunoblotted for α1-antitrypsin, EDEM1 and VCP as the loading control for the WCL where indicated.Protein quantification of EDEM1 levels presented in Figure 7G using ImageJ software for HeLa (**B**) and HuH7 cells (**C**). The bars are representative of three independent experiments and the values shown are the mean ±SEM of the respective experiments (n.s.: non-significant).

.

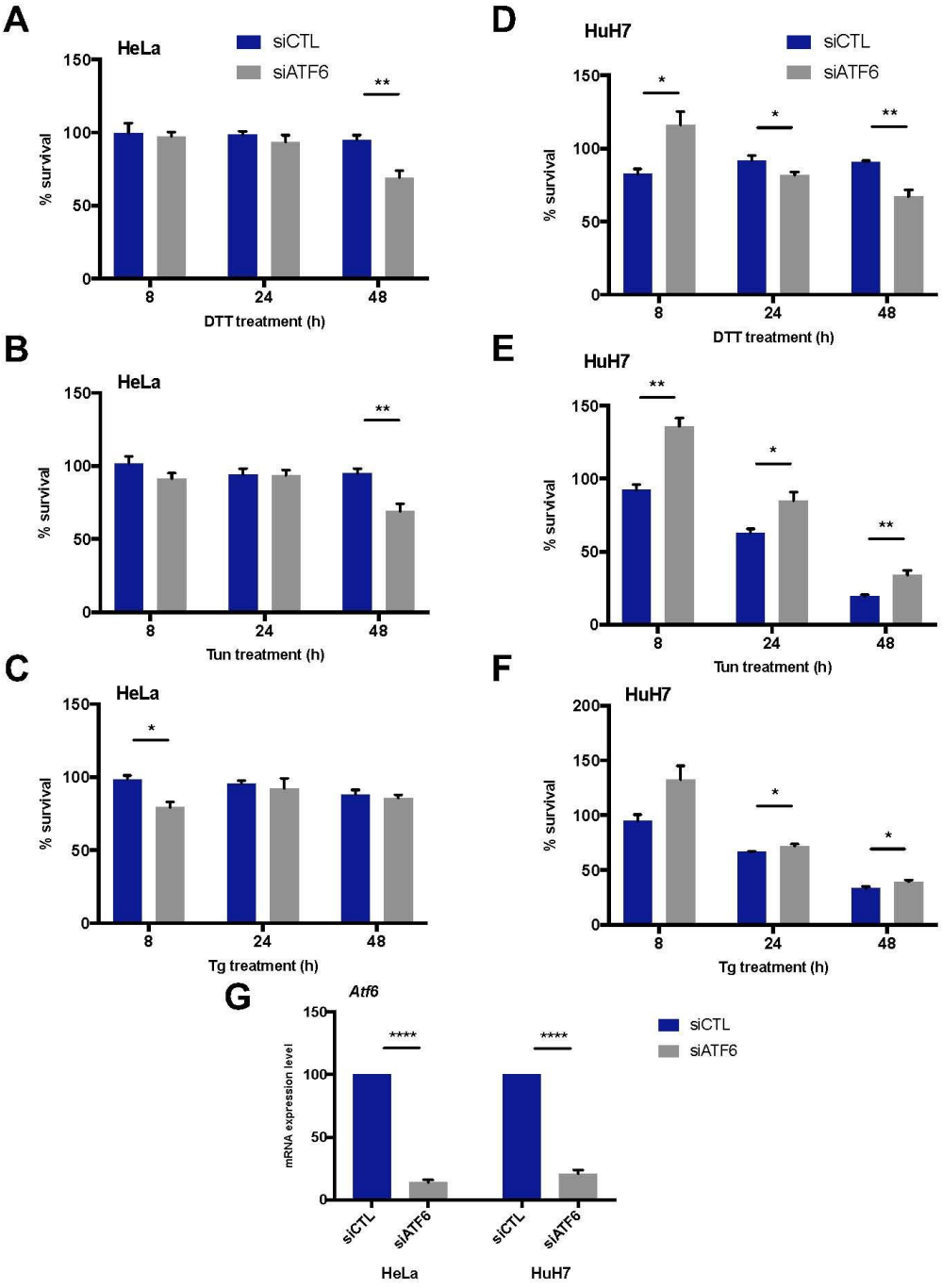

FIGURE 11. Impact of ATF6 silencing on Hela and HuH7 cells sensitivity to ER stress. (**A-C**) HeLa cells were transfected with siATF6 (25 nM) for 48 hours and then left untreated or treated with 1mM DTT (**A**) or 5µg/ml Tun (**B**) or 500nM of Tg (**C**) for 8, 24 and 48 hours. Cell survival was measured using the WST1 assay. The bars indicated are normalised to the 0h time-point or to the "non-treated cells" wells in the 96-well plates of the assay, which is expressed as 100% absorbance. (**D-F**) HuH7 cells were treated like the HeLa cells in (A-C). (**G**) qPCR for *Atf6* mRNA, after normalization to Actin mRNA expression levels. Data shown are representative of three or more independent experiments and the values shown are the mean ±SEM of the respective experiments (*p<0.05, **p<0.01, ****p<0.0001).

.